Separation Science and Technology
Publication details, including instructions for authors and subscription information:
http://www.informaworld.com/smpp/title~content=t713708471

Simultaneous Removal of Algae and Their Secondary Algal Metabolites from Water by Hybrid System of DAF and PAC Adsorption

S. H. Roh[a]; D. H. Kwak[b]; H. J. Jung[b]; K. J. Hwang[b]; I. H. Baek[c]; Y. N. Chun[a]; S. I. Kim[a]; J. W. Lee[a]
[a] Department of Chemical and Biochemical Engineering, Chosun University, Gwangju, South Korea [b] Department of Environmental and Chemical Engineering, Seonam University, Namwon, South Korea [c] Fossil Energy & Environment Research Department, Korea Institute of Energy Research, Carbon Dioxide Reduction & Sequestration R&D Center, Daejon, South Korea

To cite this Article Roh, S. H. , Kwak, D. H. , Jung, H. J. , Hwang, K. J. , Baek, I. H. , Chun, Y. N. , Kim, S. I. and Lee, J. W.(2008) 'Simultaneous Removal of Algae and Their Secondary Algal Metabolites from Water by Hybrid System of DAF and PAC Adsorption', Separation Science and Technology, 43: 1, 113 — 131
To link to this Article: DOI: 10.1080/01496390701764494
URL: http://dx.doi.org/10.1080/01496390701764494

Separation Science and Technology, 43: 113–131, 2008

ISSN 0149-6395 print/1520-5754 online
DOI: 10.1080/01496390701764494

Simultaneous Removal of Algae and Their Secondary Algal Metabolites from Water by Hybrid System of DAF and PAC Adsorption

S. H. Roh,[1] D. H. Kwak,[2] H. J. Jung,[2] K. J. Hwang,[2] I. H. Baek,[3] Y. N. Chun,[1] S. I. Kim,[1] and J. W. Lee[1]

[1]Department of Chemical and Biochemical Engineering, Chosun University, Gwangju, South Korea
[2]Department of Environmental and Chemical Engineering, Seonam University, Namwon, South Korea
[3]Korea Institute of Energy Research, Fossil Energy & Environment Research Department, Carbon Dioxide Reduction & Sequestration R&D Center, Daejon, South Korea

Abstract: The feasibility of a hybrid system consisting of powdered activated carbon (PAC) adsorption and dissolved air flotation (DAF) processes was examined for the simultaneous removal of algae (*anabaena* and *mycrocystis*) and their secondary algal metabolites (2-methylisoboneol and geosmin). Before studying the hybrid system, adsorption equilibrium and kinetics of organics (2-methylisoboneol and geosmin) produced from algae on three powdered activated carbons (wood-based, coal-based, coconut-based) were studied. The flotation efficiency of algae and PAC in DAF process was evaluated with zeta potential measurements. Interestingly, we found that the agglomerate of bubble and PAC particle can be successfully floated by DAF. In addition, the simultaneous removal of algae and organics (i.e., secondary algal metabolites) dissolved in water can be achieved by using the hybrid system of adsorption/DAF processes.

Keywords: Adsorption, DAF, algae, MIB, geosmin, hybrid process

Received 1 January 2007, Accepted 29 July 2007

Address correspondence to I. H. Baek and J. W. Lee, Korea Institute of Energy Research, Fossil Energy & Environment Research, Department, Carbon Dioxide Reduction & sequestration R & D Center, Daejon 305-343, South Korea and Department of Chemical and Biochemical Engineering, Chosun University, Gwangju 501-759, South Korea. E-mail: ilhbaek@kier.re.kr or jwlee@chosun.ac.kr

INTRODUCTION

Many reservoirs have been constructed in Korea to store water as the geomorphologically steep slope of the land causes stream and river waters to flow out rapidly (1). The source waters in reservoirs generally contain algal particles with low density because of eutrophication. The particles are hardly removed in the conventional gravity sedimentation (CGS) unit due to their folats. Actually, many conventional water treatment plants in Korea that apply CGS have undergone serious operational problems because of the scum caused by algae floats. Recently, several large water treatment plants such as the Wonju plant ($230{,}000\ m^3\ day^{-1}$) and the Jeonnam plant ($200{,}000\ m^3\ day^{-1}$) adopted the DAF process. More recently, the presence of the musty-earthy taste and odor algal metabolites, 2-methylisoborneol (MIB) and geosmin, in water treatment brought complaints from consumers. It has been generally known that MIB and geosmin are detected by consumers as musty-earthy odors at levels as low as $10\ ng\ l^{-1}$ (2). Higher doses of PAC were required to produce acceptable quality water when the presence of algae was high during the heavy rainfalls (3). However, removing the spent PAC from water is a drawback.

On the other hand, it has been known that dissolved air flotation (DAF) is an effective solid/liquid separation process for low density particles such as algae, color, clay flocs produced from low turbidity water (4). However, DAF is limited in removing the secondary algal metabolites dissolved in water (5). A DAF unit consists of four steps: coagulation and flocculation prior to flotation, bubble generation, bubble-floc collision and attachment in a mixing zone, and rising of bubble-floc agglomerates in a flotation tank (6). If a bubble-PAC particles collision results in successful attachment, and if the resulting bubble-particle agglomerate is positively buoyant, the agglomerate can rise to the top of the liquid column and collect in a foam layer which can subsequently be skimmed off. In other words, when the PAC can be floated by DAF, a combination of DAF and PAC adsorption seems to be successfully applied in water and wastewater treatment. Many studies have been conducted on the individual process of PAC adsorption of MIB and geosmin, and DAF for algae removal (2, 3, 4–7). However, little has been known about combining the two processes systematically.

Therefore, this study focuses on the flotation removal of algae and PAC for the simultaneous removal of algae (*anabaena* and *mycrocystis*) and their secondary metabolites (MIB and geosmin) produced from algae in drinking water treatment. Prior to the studies on the hybrid system, adsorption equilibrium and kinetics of secondary metabolite organics were investigated using three types of powdered activated carbons (wood-based, coal-based, coconut based). The zeta potential measurements were conducted for algae as well as PACs with and without adsorption of the secondary algal metabolites.

EXPERIMENTAL

The adsorption experiments were carried out using two organic compounds (2-MIB and geosmin) purchased from Aldrich Co. (USA). Their chemical structures and other properties are listed in Table 1. The concentration of organics was measured by GC/MS. Three different PACs, namely, wood based (WB), coconut-shell based (HA), and coal based (CB), were obtained from James Cumming & Sons Pty Ltd. (Australia). The powdered activated carbon was rinsed with distilled water, boiled for 3 hr in distilled water, then dried at 393 K for 5 hr, and stocked inside the desiccator. To obtain the important physical properties of PACs, nitrogen adsorption-desorption isotherms were carried out using an ASAP 2010 volumetric adsorption apparatus (Micrometrics) at 77.4 K. The particle size distribution of the PACs was analyzed using a particle analyzer (ASAP 2012 Micropore, Micrometrics, USA). The surface of PACs was examined using a JSM-5400 (Japan) scanning electron microscope (SEM).

Adsorption experiments of MIB and geosmin were conducted by adding different amounts of PAC into the solution. After shaking in a constant temperature incubator at constant temperature (298.15 K) for 3 days to give sufficient contacting time for equilibrium, samples were taken from the flask and filtered through 150 mm filter paper (ADVANTEC, Japan). The filtrate was then measured for organic concentrations. The adsorption capacity (q) of PAC was determined by $q = V(C_0 - C)/m$ where C_0 and C are the initial and equilibrium (or residual) liquid-phase concentrations (mol m^{-3}), respectively, V is the volume of solution (m^3), and m is the weight of dry activated carbon (kg). On the other hand, adsorption kinetic experiments were conducted in a Carberry-type batch adsorber ($1.0–2.0 \times 10^{-3}$ m^3) at 300 rpm to obtain the concentration decay curves as a function of time.

Cells of algae, *anabaena* and *mycrocystis*, were obtained from water resources corporation (Korea). Cultivation was conducted using a medium

Table 1. Chemical properties of MIB and geosmin

	2-MIB	Geosmin
Name	2-methyl-isoborneol	Trans-1,10-dimethyl-trans-9-decalol
MW	168	182
Chemical fomular	C_7H_5OCl	$C_{12}H_{22}O$
Chemical structure	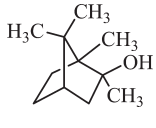	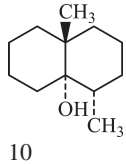
OTC (ng L^{-1})[a]	30	10
Odor	Musty Camphorous	Earthy-musty

[a]Odor threshold concentration.

which contained per liter: 1.5 g $NaNO_3$, 0.039 g K_2HPO_4, 0.075 g $MgSO_4 \cdot 7H_2O$, 0.021 g Na_2CO_3, 0.027 g $CaCl_2$, 0.058 g $Na_2SiO_3 \cdot 9H_2O$, trace elements solution, and Fe-EDTA solution. Trace solution contained per 500 ml: 2.86 g H_3BO_3, 1.81 g $MnCl_2 \cdot 4H_2O$, 0.222 g $ZnSO_4 \cdot 7H_2O$, 0.391 g $Na_2MoO_4 \cdot 2H_2O$, 0.079 g $CuSO_4 \cdot 5H_2O$ and 0.049 g $Co(NO_3)_2 \cdot 6H_2O$. The Fe-EDTA solution was prepared by mixing 0.05 g of EDTA and 0.30 g of $FeSO_4 \cdot 7H_2O$ in 500 ml. 350 ml of medium was added to each 500 ml Erlenmeyer flask equipped with a guaze stopper and autocleave. The flasks were irradiated with UV light for 2 hr before cells were added into, and placed on a thermostat shaker. The temperature was controlled at 25°C, and the speed of the shaker at 80 rpm. 350 ml of medium was added to each 500 ml Erlenmeyer flask. Cultivation flasks were shaken for 20 days with illumination of solar light for 15 hr each day. Cells were dried under vacuum state for further experiments. Figure 1 shows SEM photos of *anabaena* and *mycrocystis*.

Prior to sedimentation and DAF operation, coagulation of algae and PAC was conducted on a Jar-Test apparatus using polyaluminium chloride as a coagulant. 10 ∼ 50 mg of coagulant and 3 ml of NaOH (0.1 M) were added

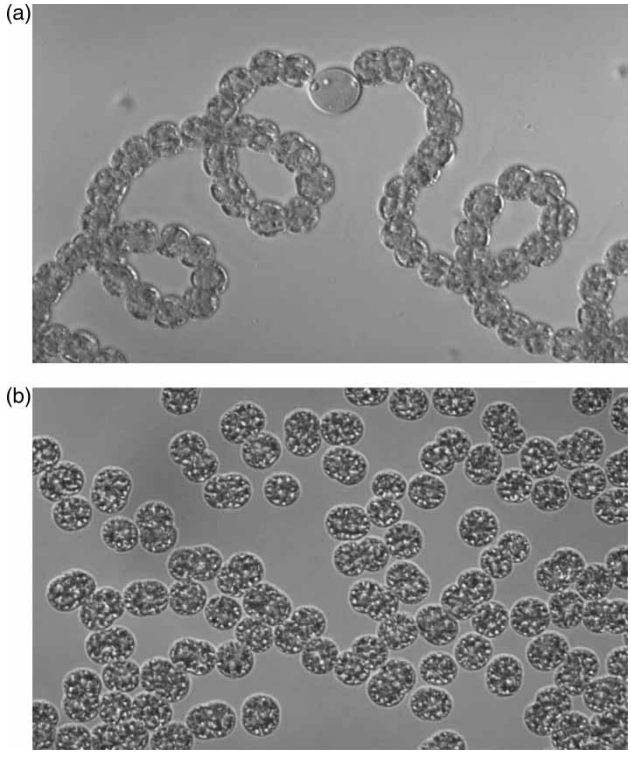

Figure 1. SEM photos of algae; (a) *anabaena*, (b) *microcystis.*

to the distilled water or raw water (1 L) and rapidly mixed (150 rpm) for 1 min followed by slow mixing (50 rpm) for 20 min. The quality of raw water (Dong-Hwa Dam, Korea) used is listed in Table 2. The pH was adjusted by adding HCl or NaOH. The supernatant after the treatment was examined for residual algae and PAC concentration. Zeta potential (Photal Otsuka ELS-8000, Japan) was measured to examine the underlying surface charge to obtain further insight in the mechanism of removal.

The schematic diagram of the DAF apparatus is shown in Fig. 2. Several DAF and CGS experiments were carried out under the operating conditions as listed in Table 3. The diameter of the flotation column made of plexiglass was 10 cm, and the height was 30 cm. Algae particles both in the presence and absence of PAC were suspended initially in the column, then bubbles were introduced in the column from the bottom side of the column. The dissolved air solution was fed into the flotation column and the particles in the column were removed by the rising bubbles. The mean diameter of the bubbles fed into the column was 25 μm. After all the bubbles in the cell reached the top of the column, the solution was sampled to obtain the flotation efficiency. The turbidity was measured using the turbidity meter (HACH 2100P).

RESULTS AND DISCUSSION

Characterization of PACs

PACs used in this study was commercially available, but its physical and chemical properties can not be obtained in detail. The surface area was calculated by using the BET method, and the pore size distribution was measured by BJH (Barrett, Joyner and Halenda) method using the nitrogen desorption data (Fig. 3a). The surface area was found to be 882 to 1200 $m^2\ g^{-1}$, and the average pore diameter was 24 to 31 Å, which belongs to the mesopore range (Figure 3b). Information on the particle size distribution of the PACs

Table 2. Characteristics of raw water

Parameters	Unit	Average values
pH	—	7.2
BOD	$mg\ L^{-1}$	0.7
COD	$mg\ L^{-1}$	2.3
SS	$mg\ L^{-1}$	1.5
DO	$mg\ L^{-1}$	10.4
Alkalinity (as $CaCO_3$)	$mg\ L^{-1}$	1.5
T-N	$mg\ L^{-1}$	1.149
T-P	$mg\ L^{-1}$	0.005

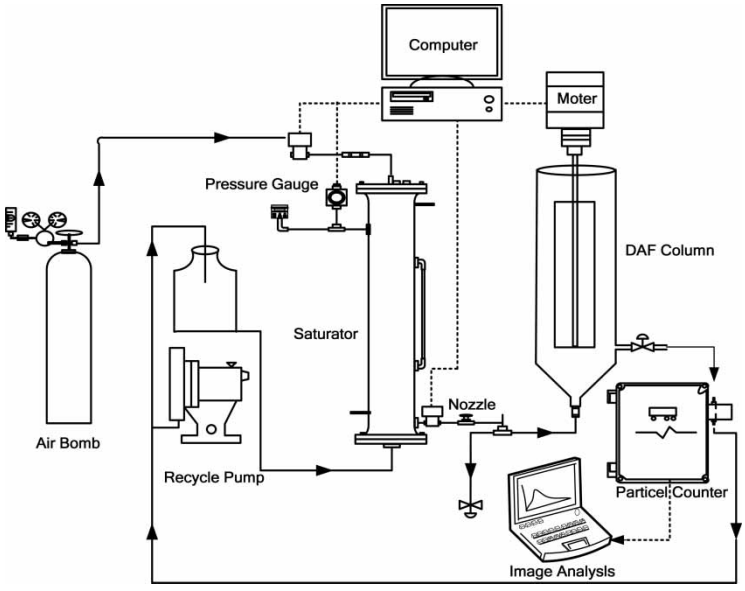

Figure 2. Schematic diagram of DAF apparatus.

used is very important, especially when it is used in conjunction with DAF. As seen in Fig. 4, the average particle size of three PACs was in the range of 11 to 34 μm. SEM images reveal that WB has a pin-like shape and the other two PACs (CB and HA) have different shapes (Fig. 5). The physical properties of the three PACs determined in this work are listed in Table 4.

Adsorption Study

It is meaningful to investigate how much concentration of PAC (i.e., dose) is required to remove dissolved organics by PAC adsorption in water treatment. Removal efficiency of suspended solids by DAF process is highly related with

Table 3. Experimental conditions for CGS and DAF

Step	Items	Values
Rapid mixing	Paddle speed (rpm)	150
	Time (min)	1
Slow mixing	Paddle speed (rpm)	50
	Time (min)	20
CGS	Sedimentation (min)	30
DAF	Recycle ratio (%)	20
	Saturator pressure (kg cm^{-2})	5

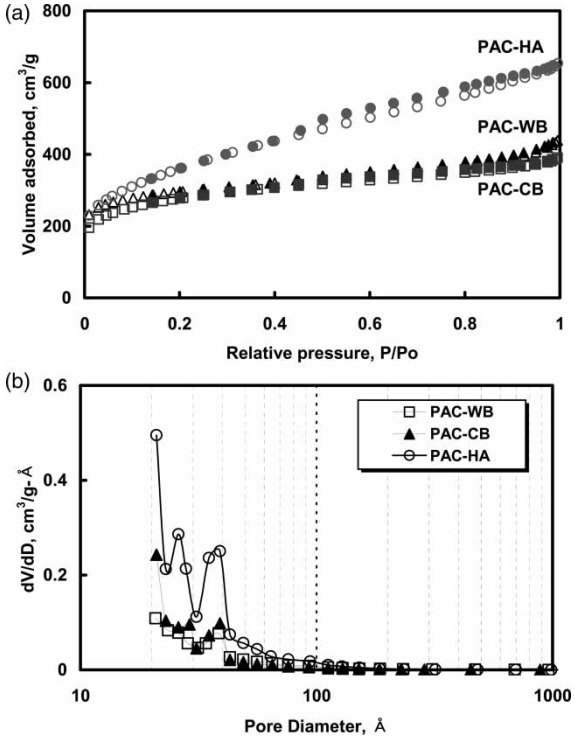

Figure 3. Results of (a) nitrogen adsorption and desorption isotherms and (b) pore size distribution of PACs.

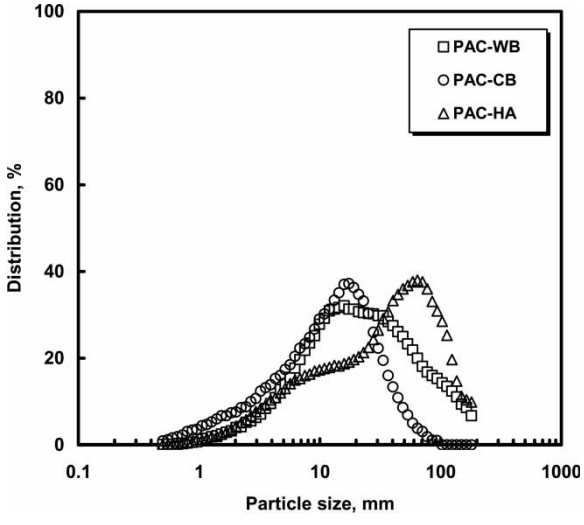

Figure 4. Particle size distribution of PACs.

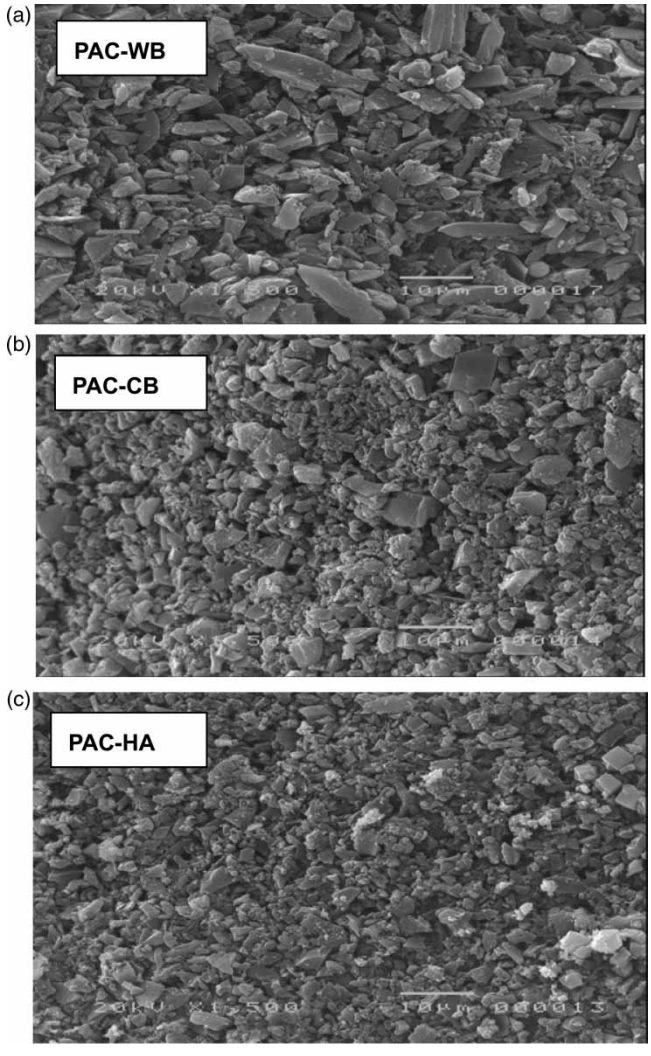

Figure 5. SEM photos of PACs; (a) PAC-WB, (b) PAC-CB, (c) PAC-HA.

the concentration of solids (i.e., turbidity). Prior to the studies on the hybrid system of adsorption and DAF, adsorption equilibrium and kinetics of two organics (MIB and geosmin) were investigated. Adsorption isotherms of PACs used in this work were the most important information for estimating carbon dose for the removal of MIB and geosmin (2, 3). The adsorption capacity mainly depended on the properties of the adsorbate and adsorbent. From our previous experimental results, the adsorption capacity of geosmin was found to be much higher than that of MIB for the same PACs at constant temperature (298.15 K). In addition, MIB and geosmin were

Table 4. Characteristics of powdered activated carbon (PAC)

Specification	PAC-WB	PAC-CB	PAC-HA
Raw material	Wood-based	Coal-based	Coconut-based
BET surface area, $m^2\ g^{-1}$	882	915	1,200
Moisture content, %	5	8	10
Bulk density, kg m^{-3}	340	200	425
Mean pore diameter, Å	31	24	31
Mean particle diameter, μm	20	11	34

successfully removed using PACs at levels as low as 10 ng/l. The adsorption capacity for MIB and geosmin was the order of PAC-HA > PAC-WB > PAC-CB because PAC-HA has higher surface area (Table 4). Therefore, PAC-HA was chosen to study the adsorption equilibrium and kinetics of MIB and geosmin. Figure 6 shows the adsorption isotherms of two sorbates (MIB and geosmin) on PAC-HA. The greater affinity of geosmin compared to MIB can be attributed to its chemical structure and solubility (Table 1). This is in agreement with the results reported by Cook et al. (2) and Graham et al. (3). In general, it has been known that the adsorption capacity on activated carbon is enhanced by increasing the molecular size and aromaticity, and by decreasing solubility, polarity, and carbon chain branching. Geosmin has a slightly lower solubility and molecular weight

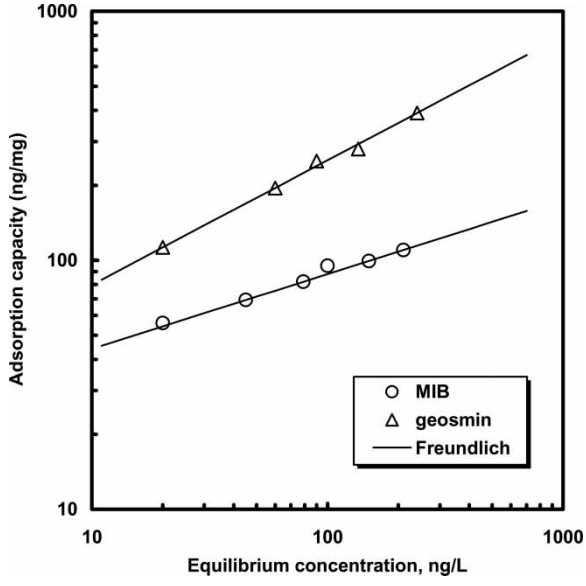

Figure 6. Adsorption isotherm of MIB and geosmin at 298.15 K.

and has a flatter structure (Table 1), which may make it easier for the adsorption in the slit-shaped pores of the activated carbon. The solid lines (Fig. 6) are the predicted results with the Freundlich isotherm. Among the well-known isotherms such as Langmuir, Freundlich, and Sips isotherm models, the Freundlich model ($q = kC^{1/n}$) described more satisfactorily the adsorption of the two organic sorbates studied. The isotherm parameters were determined by minimizing the mean percentage deviations between the experimental and the predicted amounts adsorbed. The determined isotherm parameters are $k = 22.1$, $1/n = 0.303$ for MIB and $k = 25.2$, $1/n = 0.501$ for geosmin.

To determine the contact time between the adsorbate and the adsorbent, the understanding of external and internal mass transfer coefficients within porous activated carbon is an important task. Especially, internal mass transfer is usually the rate-controlling step in most adsorption processes (8, 9). Assuming that surface diffusion is the dominant mechanism of the intraparticle mass transfer, a governing model equation with initial and boundary conditions is obtained as listed in Table 5. The model equations were solved numerically by applying orthogonal collocation to discretize the model equations. The discretization was done for the spatial variable, resulting in a set of ordinary differential equations with the adsorbate concentrations as the dependent variable. These equations are solved on a personal computer using a FORTRAN Compiler in double precision and LSODI of the international Mathematics and Science Library (IMSL). The detailed description on the diffusion model equations and the numerical technique to solve model equations are given elsewhere (10, 11). Among the various methods of determining the internal diffusion coefficient, the most general method is to compare the experimental concentration decay curves and the predicted values using the specified model. The experimental adsorption kinetics data for MIB and geosmin were predicted by a homogeneous surface diffusion model. Figure 7 illustrates the concentration decay curves of MIB and geosmin on PAC-HA in a batch adsorber. The solid lines in Fig. 7 are the predicted results obtained by employing a surface diffusion model. The determined external mass transfer coefficient and internal surface diffusivities of MIB are $6.26 \times 10^{-5}\,\mathrm{m\,s^{-1}}$ and $2.59 \times 10^{-14}\,\mathrm{m^2\,s^{-1}}$, and those of geosmin are $2.84 \times 10^{-5}\,\mathrm{m\,s^{-1}}$ and $4.71 \times 10^{-15}\,\mathrm{m^2\,s^{-1}}$. The results

Table 5. Adsorption model equation with initial and boundary conditions

Description	Equation
Surface diffusion model	$\frac{\partial q}{\partial t} = D_s\left(\frac{\partial^2 q}{\partial r^2} + \frac{2}{r}\frac{\partial q}{\partial r}\right)$
Initial condition	$q\,(r,t=0) = 0$
Boundary conditions	$\frac{\partial q}{\partial r}\Big\|_{r=0} = 0 \quad D_s\rho_p\frac{\partial q}{\partial r}\Big\|_{r=R} = k_f(C - C_s)$

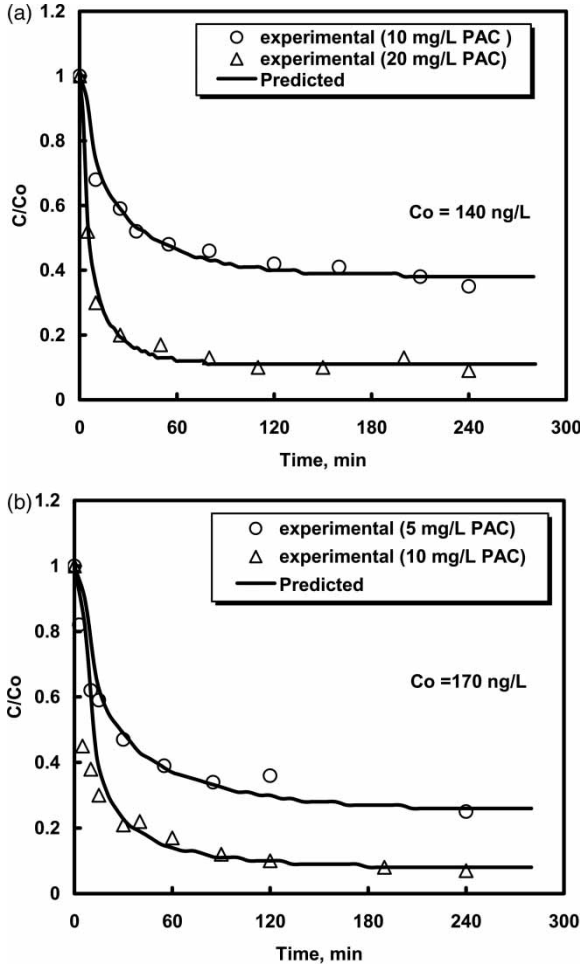

Figure 7. Adsorption kinetics of (a) MIB and (b) geosmin.

showed that the model predictions were in very good agreement with the experimental data.

DAF Study

Zeta potential is a key parameter of the double layer repulsion for individual particles, and it can be used to interpret the trend of coagulation efficiency. It has been known that colloidal particles should have zero net surface charge (isoelectric point, IEP) for agglomeration (12, 13). This can result from the adsorption of hydrogen ions or positive-charged ions (i.e., such as aluminum ions), on negatively-charged surfaces. When the zeta potential of particles is

approaching zero, the coagulation efficiency is generally improved. The coagulation mechanism of PAC is thought to be complex and involves several reaction routes, including charge neutralization (electrostatic interaction) and complex formation between PAC and alumino precipitates, adsorption, bridge formation, and surface precipitation on alumino hydroxide solid precipitate (14). In addition, it has been addressed that pH is one of the most important parameters in the coagulation processes. Depending on the pH values, the interfacial properties and reaction routes may be different.

The results of zeta potential measurements of PACs are shown in Figs. 8–10 under various experimental conditions, including the effects of water properties (distilled water and reservoir water), coagulant dose (5–20 mg L^{-1}), and

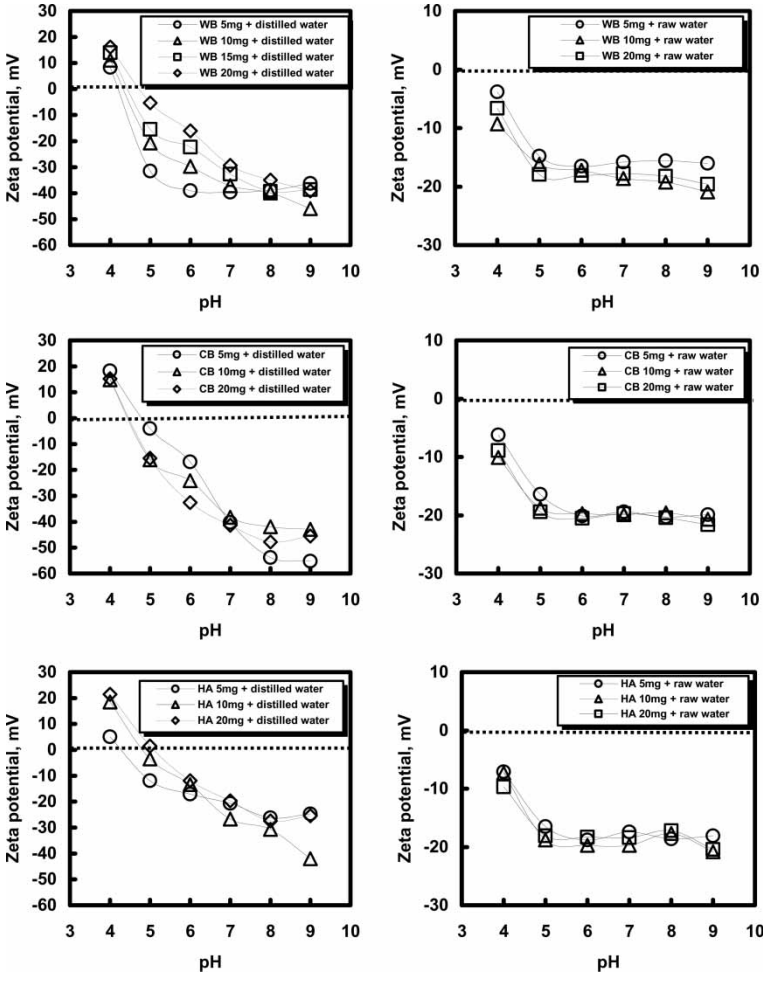

Figure 8. Zeta potential of PACs both in distilled and reservoir water.

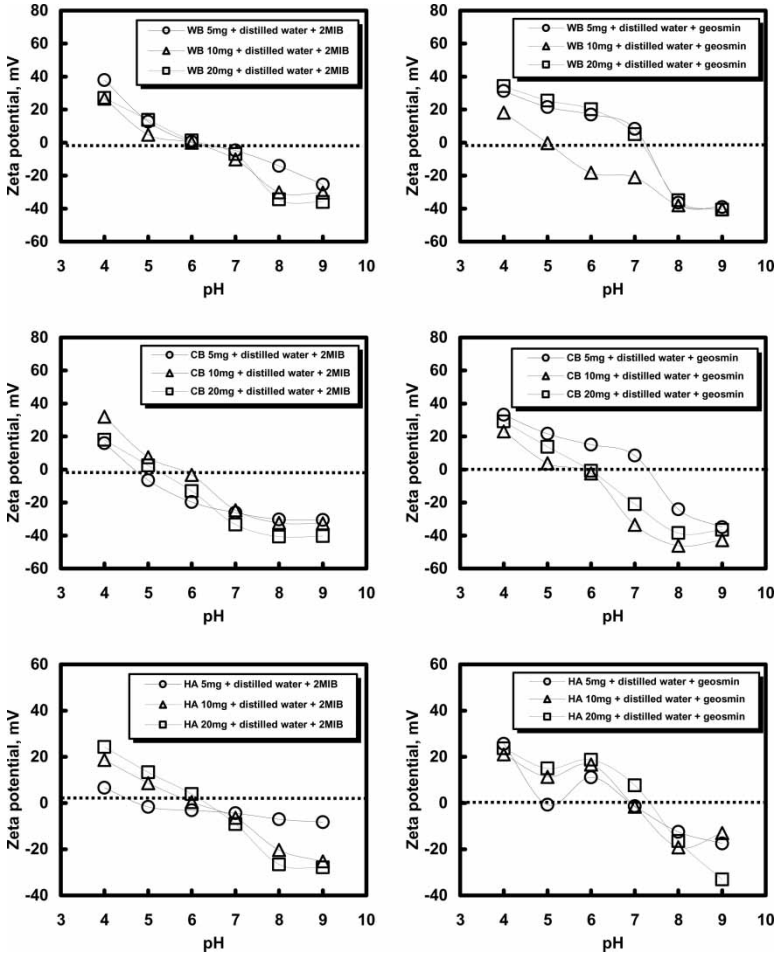

Figure 9. Zeta potential of PACs after adsorbing (a) MIB and (b) geosmin.

organic adsorption on PACs. The characteristics of reservoir water (Dong-Hwa Dam, Korea) are listed in Table 2. Figure 8 shows the variation of zeta potential of PACs depending on the water properties in terms of solution pH ($4 \sim 9$) with PACs dose (5, 10, 20 mg L^{-1}). The zeta potential values ranged approximately between $+20$ to -50 mV for distilled water and always negative values (-3–-20 mV) for reservoir water. The zeta potential decreased with an increasing PAC dose and pH. However, it was observed that the influence of the type and dose of PACs on the variation of zeta potential was quite low (Fig. 8). IEP of PACs dissolved in reservoir water was not seen while that in distilled water was present in the pH range of 4 to 5. Figure 9 shows the variation of zeta potential depending on organics (MIB and geosmin) adsorption on PACs.

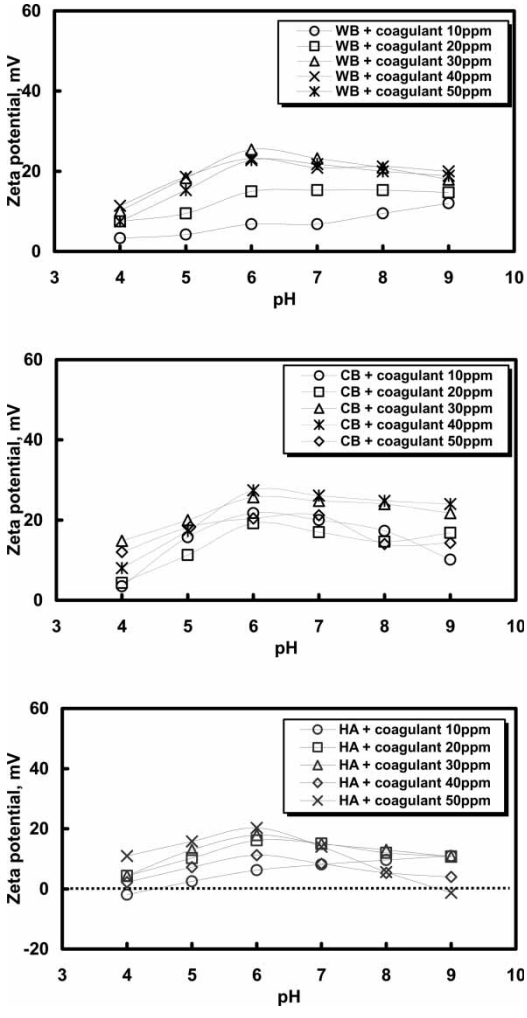

Figure 10. Zeta potential of PACs depending on coagulant dose.

The values ranged approximately between +40 to −40 mV in terms of solution pH (4–9) with PACs dose (5, 10, 20 mg L^{-1}). It was observed that IEP moved to the neutral range (pH 6–7) after adsorbing organics. This result implies that the organic adsorption affects the zeta potential of PACs.

The optimal coagulant condition is the function of the type of algae, coagulant dose, and other operating conditions such as turbidity, pH, and temperature. Polyaluminum chloride was used for altering the surface charge of PAC and algae. Figure 10 shows the variation of zeta potential of PACs depending on the coagulant dose (10–50 mg L^{-1}) and pH (4 ∼ 9). As expected, the values increased with the coagulant dose. Also, the surface charge of the PAC

particles dissolved in water was easily controlled by the adjustment of coagulant doses. In general, the particles were negatively charged in water and bubbles were also negatively charged. In this case, the removal efficiency by DAF was very low without adjustment of the surface charge of the particles. Thus, the surface charge of PAC should be changed to neutral or positive to float in the DAF process because PAC is negatively charged without coagulant doses.

Figure 11 shows the variation of zeta potential of two algae in terms of solution pH of 4∼9 with a coagulant dose of 10∼50 mg L^{-1}. It was observed that the zeta potential increased much with a coagulant dose at lower pH (4–6), while it moderately increased at higher pH (7–9). The values of zeta potential ranged between approximately $-15 \sim +25$ mV, and they were slightly different according to the types of algae. The values were $-15 - +23$ mV for *anabaena* and $-3 - 25$ mV for *microcystis*.

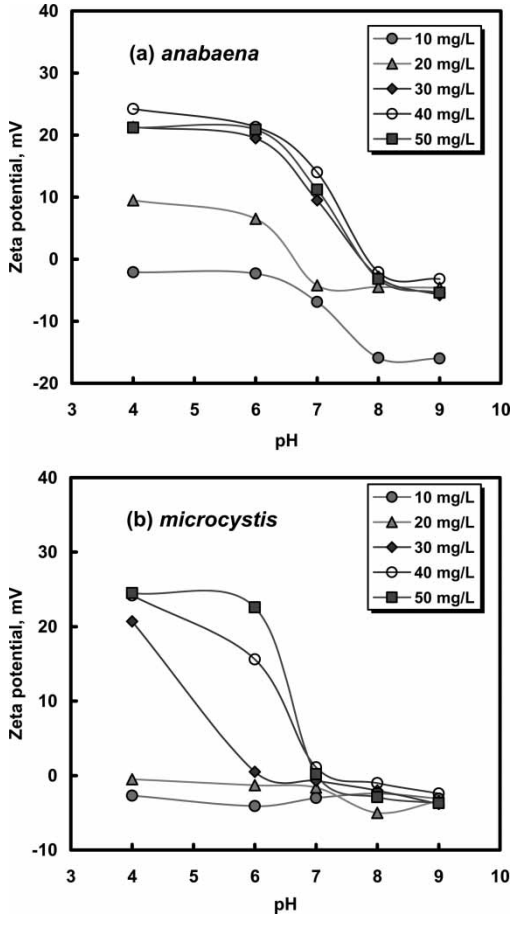

Figure 11. Zeta potential of algae depending on coagulant dose.

Unlike the results of PACs, the zeta potential of algae was quite different depending on the solution pH and coagulant dose. The turbidity removal efficiencies of *anabaena* and *microcystis* by DAF and CGS in terms of coagulant dose (10–50 mg L^{-1}) at pH 6 are shown in Fig. 12. The removal efficiency of two algae increased with coagulant dose although its tendency was changed when the coagulant dose was over 40 mg L^{-1}. We believe that DAF is an effective method of removing algae.

On the other hand, the removal efficiency of three types of PACs was compared in the absence and presence of coagulant in order to verify the DAF methodology to float PACs (Table 6). CGS results were included for comparison. The removal efficiency without coagulation was very low (<10%), while with increasing coagulant dose the efficiency increased up

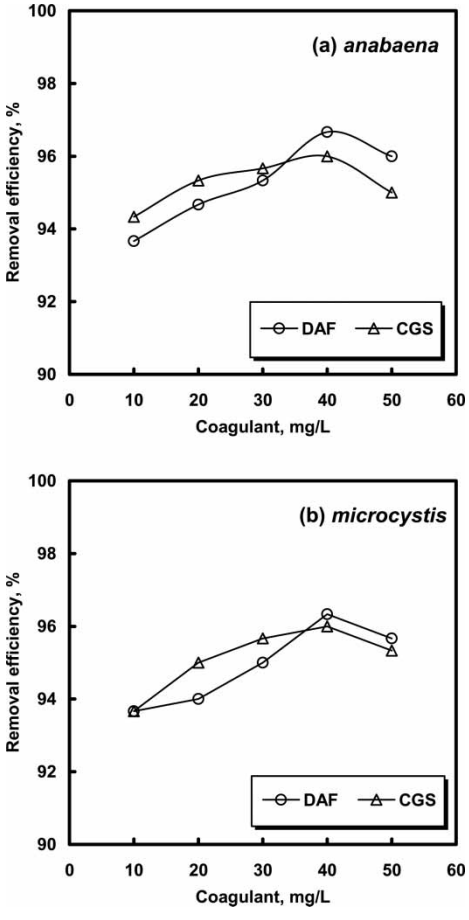

Figure 12. Removal efficiency of algae by DAF and CGS depending on coagulant dose.

Table 6. Removal efficiency of PACs by sedimentation and DAF (unit:%)

	Without coagulant		With coagulant	
PAC[a]	Sedimentation	DAF	Sedimentation	DAF
PAC-CB	1.7	9.7	77.5	94.6
PAC-WB	3.8	5.3	72.9	94.2
PAC-HA	1.5	6.0	69.5	93.6

[a]Conditions: PAC (10 mg L^{-1}), coagulant (polyaluminum chloride, 30 mg L^{-1}).

to 70% by CGS and up to 95% by DAF. We found that the electrostatic interactions between positively charged algal particles and negatively charged bubbles became mutually attractive when the coagulant was used. However, the interactions between algal particles and bubbles are repulsive without the use of the coagulant. It was also found that the removal efficiency was almost independent of the types of PAC as listed in Table 6. On the other hand, the removal efficiency of algae in the absence and presence of PAC was examined (Table 7). The initial concentrations of *anabana* and *mycrosystis* were 6.9×10^4 and 5.2×10^5 cells mL^{-1}. Results showed that the removal efficiencies of *anabana* and *mycrosystis* were very high about 94–96% regardless of the presence of PAC when a coagulant of 35 mg L^{-1} was used at solution pH 6. In addition, MIB and geosmin can be simultaneously removed using HA-PAC. This result implies that DAF is an effective process for the simultaneous removal of algae and their secondary metabolites (MIB and geosmin). On the basis of this finding, therefore, we believed that the simultaneous removal of algae and PAC adsorbing the secondary algal metabolites can be successfully achieved by employing the hybrid system of PAC adsorption and DAF processes for water and wastewater treatments.

Table 7. Removal efficiency of algae and their secondary metabolites by DAF with and without PAC (unit:%)

	Without PAC	With PAC[a]
Anabana	96	94
Mycrocystis	96	95
2-MIB	2	92
Geosmin	5	98

[a]Conditions: PAC-HA (20 mg L^{-1}), adsorption time (50 min), coagulant (polyaluminum chloride, 35 mg L^{-1}), initial concentration of *anabana* (6.9×10^4 cells mL^{-1}), initial concentration of *mycrosystis* (5.2×10^5 cells mL^{-1}), initial concentration of 2-MIB (26 ng L^{-1}), initial concentration of geosmin (31 ng L^{-1}).

CONCLUSIONS

This study demonstrated that algae (*anabaena* and *mycrocystis*) and their secondary metabolites (2-MIB and geosmin) dissolved in water can be successfully removed by DAF technique. The zeta potential values of algae and PAC increased with coagulation dose, and the flotation efficiencies were also enhanced. The removal efficiency of PACs was very low without coagulation, while the efficiency increased up to 70% by CGS and to 95% by DAF when coagulant (i.e., polyaluminium chloride) was used. The removal efficiencies of algae by DAF or CGS were very high both in the absence and the presence of PAC. Our experimental results suggest that the hybrid system consisting of powdered activated carbon (PAC) adsorption and dissolved air flotation (DAF) processes can be widely used for the simultaneous removal of algae and PAC adsorbing the secondary algal metabolites dissolved in water.

ACKNOWLEDGEMENT

This work was supported by Grant No. R01-2004-000-11029-0 from the Korea Science and Engineering Foundation. One of us (Chun) acknowledges the support by a grant from the Korea Science Foundation (No. R-01-2006-000-10355-0) with funds provided by the Ministry of Science and Technology in 2006.

REFERENCES

1. Kwak, D.H., Jung, H.J., Kim, S.J., Won, C.H., and Lee, J.W. (2005) Separation characteristics of inorganic particles from rainfalls in dissolved air flotation: a Korean perspective. *Separation Science and Technology*, 40: 3001–3016.
2. Cook, D., Newcombe, G., and Sztajnbok, P. (2001) The application of powdered activated carbon for MIB and geosmin removal: predicting PAC doses in four raw waters. *Wat. Res.*, 35: 1325–1333.
3. Graham, M., Summers, R., Simpson, M., and Maceleod, B. (2000) Modeling equilibrium adsorption of 2-methylisoborneol and geosmin in natural water. *Wat. Res.*, 34: 2291–2300.
4. Schulze, H.J. (1984) *Physico-Chemical Elementary Processes in Flotation*; Elsevier.
5. Okada, K., Akagi, Y., Kogure, M., and Yoshioka, N. (1990) Analysis of particle trajectories of small particles in flotation when the particles and bubbles are both charged. *Can. J. Chem. Eng.*, 68: 614–621.
6. Fukushi, K., Tambo, N., and Matsui, Y. (1995) A kinetic model for dissolved air flotation in water and wastewater treatment. *Wat. Sci. Tech.*, 32: 37–47.
7. Chen, Y.M., Liu, J.C., and Ju, Y.H. (1998) Flotation removal of algae from water. *Colloids and Surfaces B: Biointerfaces.*, 12: 49–55.

8. Ruthven, D.M. (1984) *Principles of Adsorption and Adsorption Processes*; John Wiley & Sons: New York.
9. Yang, R.T. (1986) *Gas Separation by Adsorption Processes*; Butterworths: Boston.
10. Lee, J.W., Kwon, T.W., and Moon, I.S. (2004) Adsorption of monosaccharides, disaccharides, and maltooligosaccharides on activated carbon for separation of maltopentaose. *Carbon*, 42: 371–380.
11. Lee, J.W., Jung, H.J., Kwak, D.H., and Chung, P.G. (2005) Adsorption of dichloromethane from water onto hydrophobic polymer resin XAD-1600. *Wat. Res.*, 39: 617–629.
12. Seshmukh, S.S. and Childress, A.E. (2001) Zeta potential of commercial RO membranes: influence of source water type and chemistry. *Desalination*, 140: 87–95.
13. Rebhun, M. and Lurie, M. (1993) Control of organic matter by coagulation and floc separation. *Wat. Sci. Tech.*, 27: 1–20.
14. Kim, T.H., Park, C.H., Shin, E.B., and Kim, S.Y. (2004) Decolorization of disperse and reactive dye solutions using ferric chloride. *Desalination*, 16: 49–58.